

PCCP

Accepted Manuscript



This is an *Accepted Manuscript*, which has been through the Royal Society of Chemistry peer review process and has been accepted for publication.

Accepted Manuscripts are published online shortly after acceptance, before technical editing, formatting and proof reading. Using this free service, authors can make their results available to the community, in citable form, before we publish the edited article. We will replace this *Accepted Manuscript* with the edited and formatted *Advance Article* as soon as it is available.

You can find more information about *Accepted Manuscripts* in the [Information for Authors](#).

Please note that technical editing may introduce minor changes to the text and/or graphics, which may alter content. The journal's standard [Terms & Conditions](#) and the [Ethical guidelines](#) still apply. In no event shall the Royal Society of Chemistry be held responsible for any errors or omissions in this *Accepted Manuscript* or any consequences arising from the use of any information it contains.

Role of Isomerization in Kinetics of Self-Assembly: p-Terphenyl-m-Dicarbonitrile on Ag(111) Surface

David Abbasi-Pérez and J. Manuel Recio

MALTA-Consolider Team and Departamento de Química Física y Analítica, Facultad de Química,
Universidad de Oviedo, 33006 Oviedo, Spain

Lev Kantorovich*

Physics Department, King's College London, Strand, London, WC2R 2LS, United Kingdom
lev.kantorovitch@kcl.ac.uk

Abstract

Using a toolkit of theoretical techniques comprising *ab initio* density functional theory calculations, the nudged elastic band method and kinetic Monte Carlo (KMC) modeling, we investigate in great detail how para-Terphenyl-meta-Dicarbonitrile (pTmDC) molecules diffuse and isomerize to self-assemble on the Ag (111) surface. We show that molecules “walk” on the surface via a pivoting mechanism moving each of its two “legs” one at a time. We then identify a peculiar “under-side” isomerization mechanism capable of changing the molecules chirality, and demonstrate that it is fundamental in understanding the growth of hydrogen bonding assemblies of ribbons, linkers, clusters and brickwall islands on the Ag (111) surface, as observed in recent scanning tunneling microscopy experiments (*ChemPhysChem* **11**, 1446 (2010)). The discovered underlying atomistic mechanism of self-assembly may be behind the growth of other hydrogen bonding structures of chiral molecules on metal surfaces.

Introduction

One route of building sophisticated nanodevices is to explore natural ability of many organic molecules to self-assemble on crystal surfaces into structures of various complexity varying from small clusters to ribbons and islands.¹⁻³ The structures the molecules form on surfaces are a result of a complex interplay between molecule-molecule and molecule-surface interactions, and knowing these may help in understanding many assemblies observed.⁴ However, in order to be able to manipulate the growth of molecules into desired geometries on surfaces, i.e. steer the assembly along a predefined direction to form structures most suitable for the given application, one needs to understand the mechanism of growth of the structures in detail. The latter knowledge cannot be gained just by understanding why the molecules bind to themselves and to the surface, i.e. their ability to form dimers, trimers, and bigger clusters; it requires comprehensive simulations of *kinetics of growth* which in turn necessitates understanding of diffusion mechanism, rates of transformations between different states of molecules on the surface (e.g. between various isomers) and the corresponding rates of formation of clusters of molecules and their decomposition. By means of scanning tunneling microscopy (STM) it is possible to get access to detailed information on how the molecules are organized on the surface and identify the essential building blocks predominant in the self-assembly process. However, time evolution of growth is less accessible to STM based techniques (unless the growth happens much slower than the available scan speeds), and hence theoretical investigation of the factors determining the growth becomes extremely important.

In a recent experimental study,⁵ deposition of [1,1';4',1'']-terphenyl-3,3''-dicarbonitrile (also known as para-Terphenyl-meta-Dicarbonitrile or pTmDC in short) molecules on the Ag(111) surface was investigated by STM. In the gas phase the molecules may exist either in *cis* (C) or *trans* (T) forms (isomers) shown in Fig. 1. When evaporated on the silver surface the two isomers can be clearly imaged with STM at room temperature (RT) both appearing in a similar rectangular form. Though the *cis* isomer is achiral, *trans* isomer is however prochiral, i.e. depending on which side the molecule gets adsorbed on the surface, two possibilities exist denoted L- and D-*trans*, Fig. 1.

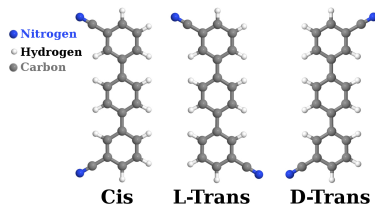


Figure 1 Cis and trans isomers of pTmDC .

Using STM, it was found⁵ that at low coverages upon thermal quenching the molecules form one-dimensional (1D) ribbons which cross with and connect to each other via a number of linkers which molecular arrangement has been resolved. At higher coverages two-dimensional (2D) islands are formed instead. When evaporated on the surface, both cis and trans isomers are expected to be present; however, intriguingly, it was claimed that mostly trans isomers were found in abundance on the surface (e.g. in ribbons) after the self-assembly takes place at either small or large coverage with cis isomers appearing only in small amounts, mostly in linkers and at the ends of the ribbons. Note that it was assumed⁵ that in all these structures the molecules bind to each other via double hydrogen bonds. The STM images revealed that both trans species form equivalent structures which are mirror reflections of each other.

In our preceding work⁶ various possible assemblies of the pTmDC molecules were studied in the gas phase using *ab initio* density functional theory (DFT) method, assuming that the role of the surface was to constrain the molecular structures in two dimensions. This method allowed to consider large molecular structures at reasonable computational expense, including many that were resolved in the experimental STM images. The hypothesis⁵ that the binding mechanism holding the molecules together on the surface is based on hydrogen (or H) bonding was also broadly confirmed, although it was found that dispersion interaction plays a significant role in the binding, especially for weak dimers. It was also established that in the gas phase there are very small barriers between cis and trans isomers, confirming that, as expected, there must be equal amounts of the two conformers during their evaporation on the surface. Hence, upon deposition, there must be 50% of cis and by 25% of each of the trans isomers.

Here we go further and consider the silver surface explicitly; moreover, we present a detailed *ab initio* density functional theory (DFT) based theoretical study of the *kinetic processes* responsible for the growth of the observed structures on the Ag(111) surface. Our main aim is to provide the driving mechanism(s) of self-assembly of pTmDC molecules on this surface at small and up to intermediate coverages. This includes detailed determination of the transition paths involved in the cis-to-trans isomerization, molecular diffusion, binding and decomposition of molecular structures, followed by extensive kinetics modeling of molecular assemblies themselves based on Kinetic Monte Carlo (KMC) technique. This comprehensive and complementary toolkit of theoretical methods is essential to build up a detailed understanding of the growth mechanism for the observed assemblies and to verify the claim⁵ stated above about the observed chiral selectivity. The corresponding energy barriers for the transitions incorporated in the KMC simulations were all calculated using Nudged Elastic Band (NEB)^{7,8} method and DFT.

Methods

DFT calculations were carried out using the CP2K code.⁹ It implements periodic boundary conditions and the hybrid Gaussian and plane wave method (GPW).¹⁰ Goedecker-Teter-Hutter (GTH)¹¹ pseudopotentials were used as well as Perdew-Burke-Ernzerhof (PBE) generalized gradient exchange-correlation functional¹² with the dispersion correction to energy and forces due to Grimme's DFT-D3 method.¹³ The optimized m-DZVP basis set¹⁴ was used for all atoms and a plane wave cutoff energy of 280 Ry. Geometries were relaxed until forces on atoms were less than 0.02 eV/Å. In all calculations (except for those with adsorbed infinite ribbons and islands) the corresponding simulation cells were chosen big enough to ensure that there are sufficient distances between images of adsorbed molecules and clusters to make the interaction between them negligible.

Binding energy of a complex $S + M_N$ obtained by placing N molecules M on the surface S is defined in the usual way as

$$E_{bind} = E_{S+M_N} - E_S^0 - \sum_{M=1}^N E_M^0,$$

where E_{S+M_N} is the DFT total energy of the complex $S + M_N$, E_S^0 is the energy of the individually relaxed surface, and E_M^0 are the energies of the individually relaxed molecules (C and/or T). Because a localized basis set is employed, the basis set superposition error (BSSE) is added to the binding energies, which is calculated by means of the (positive) counterpoise (CP) correction¹⁵ method. When considering contributions to the binding energy between molecules in a cluster which is adsorbed on the surface, we also calculated the *cluster binding energy* using

$$E_{Hb} = \left[E_{S+M_N} - \sum_{M=1}^N (\Delta E_M + E_M^0) - E_S^0 \right],$$

where $\Delta E_M = E_{S+M} - E_S^0 - E_M^0$ is the binding energy to the surface of an individual monomer M calculated at the geometry of the whole complex $S + M_N$. The energy E_{Hb} has the meaning of a mean H bonding energy between molecules on the surface.

All energy barriers were calculated by means of the Nudged Elastic Band (NEB) method.^{7,8} Both Improved Tangent NEB and the Climbing Image NEB calculations^{16,17} were employed, with the number of images varying between 7 and 9.

To illustrate the strength of H bonding interaction in a complex $S + M_N$ of N molecules on the surface, we used two methods. In the first one, we analyzed electronic density difference¹⁸⁻²⁰ (EDD) defined as $\Delta\rho(\mathbf{r}) = \rho(\mathbf{r}) - \sum_A \rho_A(\mathbf{r})$, where ρ is the total density of the complex, while ρ_A is the density of the component A (either S or M) considered in the geometry of the complex. In the second method, we analyzed the topology of the electron density using the so-called (dimensionless) reduced density gradient,²¹⁻²³ when the following quantity is analyzed:

$$s(\mathbf{r}) = \frac{1}{2} \frac{|\nabla\rho(\mathbf{r})|}{(3\pi^2)^{1/3} \rho(\mathbf{r})^{4/3}}$$

This is specially designed to identify regions where non-covalent interactions (NCI) are dominant. In visualizing $s(\mathbf{r})$, the iso-surfaces are colored on a blue-green-red color scale. With this color scheme, red indicates strong non-bonding (steric) repulsion, green indicates weak interaction such as dispersion, while blue detects strong attractive interaction such as the H bonds.

Results

Monomers on the silver surface

Knowledge of the energetics of monomers on the surface is mandatory for clear understanding of the self-assembly process. As possibilities of geometrical positions of the monomers on the surface are enormous, we carried out a systematic exploration of the potential energy landscape to reveal all possible adsorption sites (see the Supplementary Information for details). Altogether, 173 and 183 orientations of cis and trans isomers, respectively, were relaxed with our DFT method.

The most stable configurations found and their corresponding binding energies are presented in Fig. 2 for the cis and trans isomers (more relaxed geometries are shown in Figs. S2 and S3 in the Supplementary Information). It is seen from these results that both isomers are strongly bound to the silver surface with binding energies as large as 200 kJ/mol, and hence both isomers are equally favorable. Careful inspection of the obtained geometries revealed that favorable geometries have at least two common features: (i) N atoms of the molecule prefer to be located near the top of Ag atoms, showing a weakly dative covalent bonding that we call a NAS (Nitrogen Atom Surface) interaction, and (ii) phenyl rings tend to avoid Ag atoms below their centers. We also find that there is some tendency for the carbonitrile groups to bend towards the surface, so that the molecule adopts a dome-like shape seen in Fig. 3. Thus, the mean distances to the surface of the carbon skeleton of the monomers is around 3.25 Å, whereas that of the N atoms is only around 2.65 Å (see the Supplementary Information for further details). The large number of adsorption geometries found with similar binding energies and the small variation in the molecule geometry with respect to the surface suggest that the corresponding potential energy surface (PES) is weakly corrugated.

Dispersion is the essential attractive contribution to the binding energy in all stable monomers including those shown in Fig. 2. To investigate the nature of the interaction of the molecule to the surface, we analyzed in detail the electron density for a number of adsorbed monomers using both the electron density difference (EDD)¹⁸⁻²⁰ and the Non-Covalent Interaction (NCI)²¹⁻²³ methods, which give complementary results. As an example, a comparison of the plots using the two methods is shown in Fig. 3 for one representative C and one T monomer. It is clearly seen that there is a considerable binding (as the charge density excess reveals) between N atoms and the surface Ag atoms (Fig. 3 A and B). This NAS interaction justifies the preference of the molecule for certain docking sites where N atoms are on top of Ag atoms. The big green area depicted by the NCI analysis

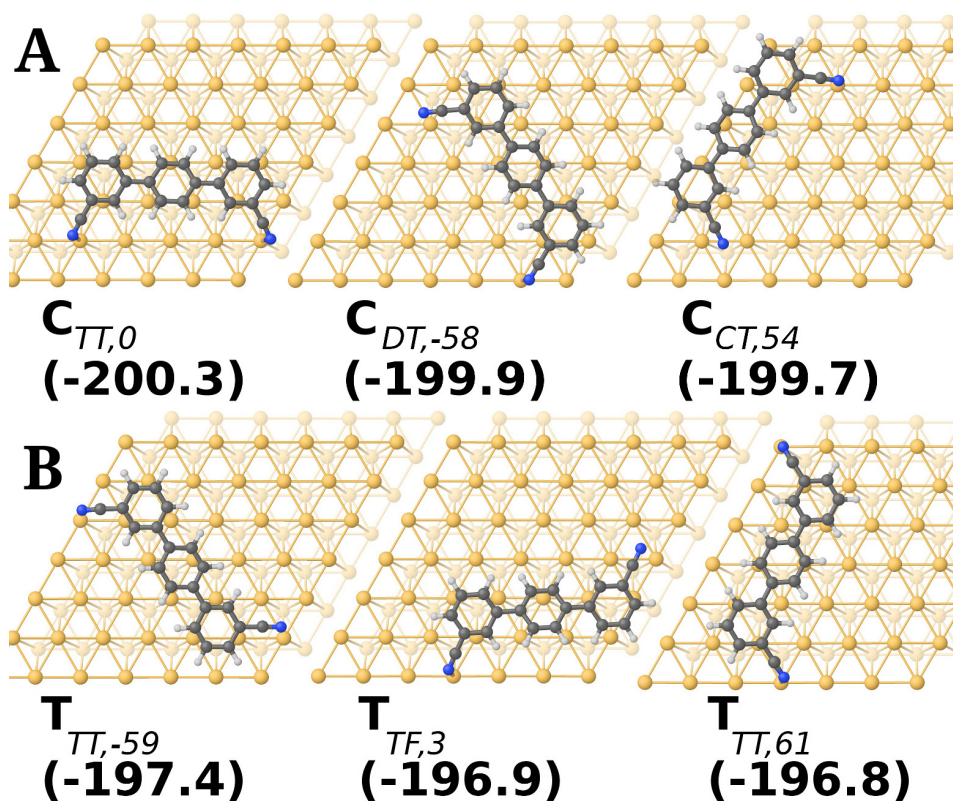


Figure 2 Three most stable (A) cis C and (B) trans T conformers on the surface found after the DFT geometry relaxation. The suggested nomenclature is meant to indicate the adsorption site and orientation of the molecule: the first subscript indicates the docking site of the left N atom, the second subscript indicates the docking site of the right N atom, and the number after the comma indicates the alpha angle (see Fig. S1 in the Supplementary Information). When both N atoms align along a vertical line, then the first subscript refers to the bottom atom. The corresponding binding energies (in kJ/mol) are also given. Only L-trans isomers are shown for clarity; the corresponding D-trans isomers with identical binding energies are obtained by appropriate flipping of the molecules (not shown).

(Fig. 3 C and D), which represents the dispersion interactions between the molecule and the surface, reveals the key role that dispersion plays in the binding mechanism, which is in agreement with the low corrugation of the PES and the large number of adsorption geometries found. Further analysis based on integrating the charge density in planes parallel to the surface revealed that there is no perceptible charge transfer between the molecule and surface. This conclusion is also confirmed by the calculated projected density of states, see Fig. S4 in the Supplementary Information.

It was suggested in the experimental study⁵ that cis-to-trans isomerization plays an essential role in the self-assembly process of the pTmDC molecules on the Ag(111) surface. Therefore, using the NEB method we have considered the isomerization reaction for one monomer geometry adsorbed on the surface. The cis-to-trans isomerization transition can be modeled by rotating around the C-C bond connecting a benzonitrile group with the central phenyl ring. This can be done in two ways: in one the benzonitrile group rotates with its N atom going round away from the surface (the *upper-side* trajectory), while in the other the group proceeds near the surface (the *under-side* trajectory). Both paths were considered using a particular pair of isomers. The initial ($T_{TF,19}$) and final ($C_{TT,23}$) geometries and the transition states in both cases along with the computed minimum energy paths (MEP) are shown in Fig. 4. It is seen that the barrier for the C→T transition of around 38.6 kJ/mol for the under-side mechanism is by about 19.3 kJ/mol lower than for the upper-side mechanism which is easily explained by the fact that in the latter case one of the N-Ag interactions needs to be broken completely, while in the former case some bonding with the surface still remains along the path. We also note that the barriers for the direct (T→C) and reverse (C→T) transitions differ by no more than 3.9 kJ/mol rendering both isomers on the surface almost equally possible, with the C isomer being marginally more favorable. Therefore, we expect C and T monomers being in almost equal amounts on the surface after first steps of deposition.

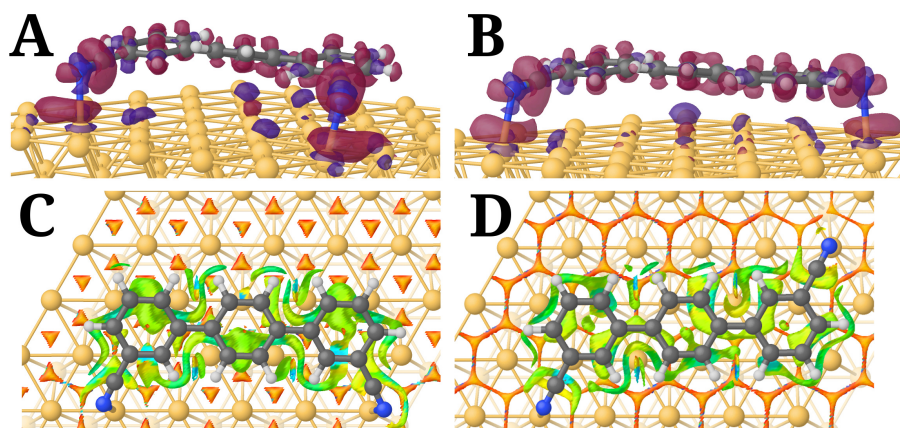


Figure 3 Comparison of the electron density difference (A,B) and NCI (C,D) plots for the cis $C_{TT,0}$ (A,C) and trans $T_{TT,1}$ (B,D) monomers adsorbed on the Ag(111) surface. In (A,B) the purple isosurface indicates an excess and the maroon depletion of the electron density, with the isosurfaces drawn at ± 0.0007 electron/ \AA^3 . The value of $s = 0.5$ was used in (C,D) for the NCI plots, see Methods for the explanation of the color scheme used.

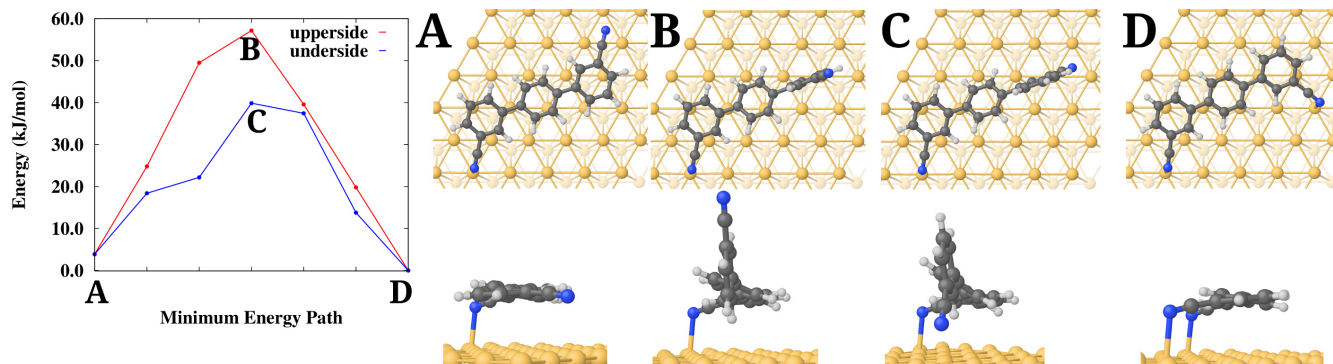


Figure 4 Cis-trans isomerization transition paths connecting the initial T (A) and final C (D) configurations via two possible mechanisms: (i) the upper-side with the transition state (B), and (ii) the under-side with the transition state (C).

Diffusion of molecules on the surface is the next necessary prerequisite for understanding their ability to assemble into structures. Using some of the nearest stable geometries as initial and final states, and applying the NEB method to calculate the transition path between them, we have investigated several diffusion paths for both C and T monomers on the surface. Two basic mechanisms were considered: (i) *sliding transition* in which the molecule loses both its N interactions to the Ag anchoring sites on the surface to move to a new stable geometry, and (ii) a two steps *pivoting transition* whereby within each step one benzonitrile group remains bonded to the surface serving as a pivot for the other group, which rotates to a new stable position. In the latter mechanism one benzonitrile group serves as a pivot during the first, while another group during the second step. Because of the very large number of adsorption geometries of monomers on the surface, calculating transitions between all possible configurations is not feasible to consider in practice. Therefore, we selected only a number of reasonable possibilities between most stable structures. Examples of both types of transitions for a C monomer together with the corresponding MEPs are shown in Figs. 5 (for a T monomer see Fig. S5 in the Supplementary Information). As expected, the sliding transition requires about 2.1-3.5 kJ/mol higher barriers to overcome for both isomers than in the pivoting mechanism. This is because during sliding two molecule-surface interactions involving two N atoms have to be simultaneously broken, whereas in the pivoting transition two steps needed for the same displacement of the molecule require each only one of these interactions to be broken at a time. Hence rather small diffusion barriers are found ranging between 1.9-3.9 kJ/mol for C and 4.8-5.8 kJ/mol for T, depending on the particular initial and final geometries.

Concluding this Section, we find that dispersion is the main interaction that binds the molecule to the surface. From the

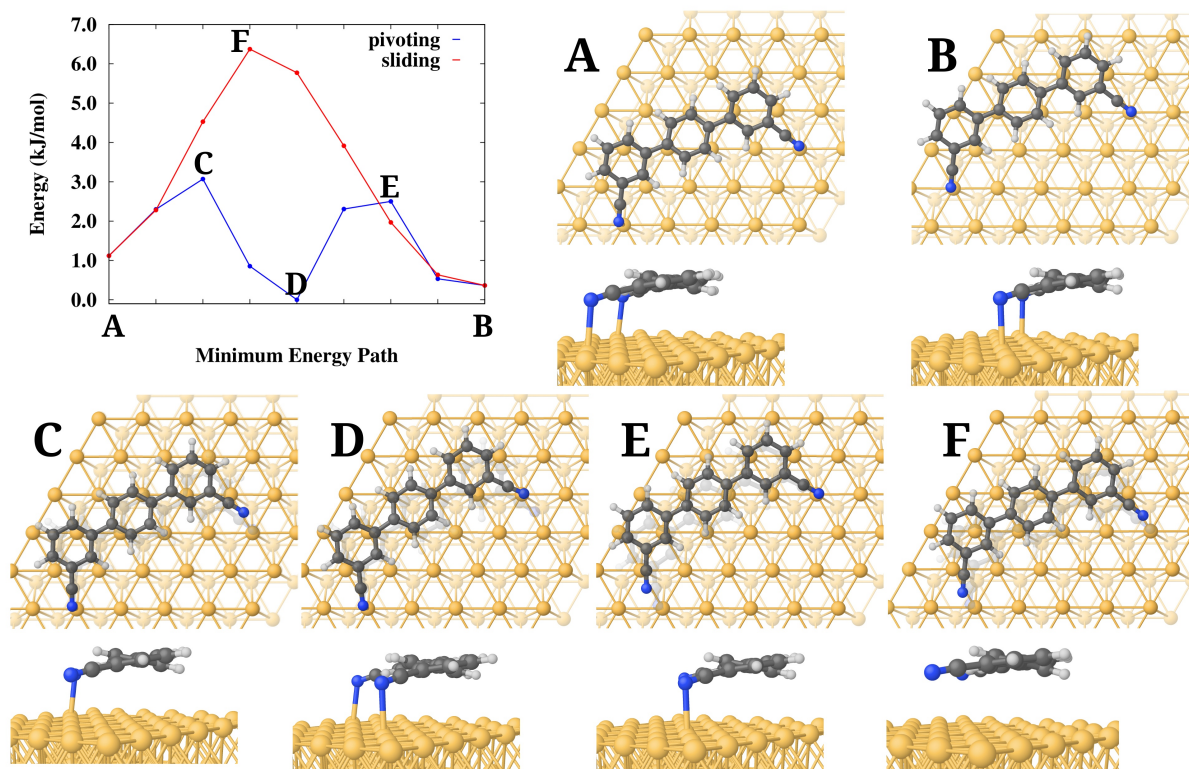


Figure 5 Diffusion paths for a C monomer on the Ag(111) surface. In the top-left panel the pivoting (blue) and sliding (red) MEP bands are shown labeled with the corresponding states shown in separate panels: initial and final (A and B), transition (C, F, E) and intermediate (D) states, as well as their geometries (top and perspective views). In the transition and intermediate states a ghost image of the molecule is superimposed showing its previous state.

large number of calculated adsorption geometries and obtained small diffusion barriers we conclude that the PES of a pTmDC molecule on the Ag(111) surface is rather flat so that the molecule must be quite mobile at RT. The preferred sites are those where favorable NAS interactions between the Ag surface with the two N are formed. Thus, the molecule can be viewed as standing on two legs. Single molecules diffuse exploiting the pivoting mechanism and C and T isomers may undergo transformations into each other following an under-side trajectory with relatively high and equal rates.

Dimers on the silver surface

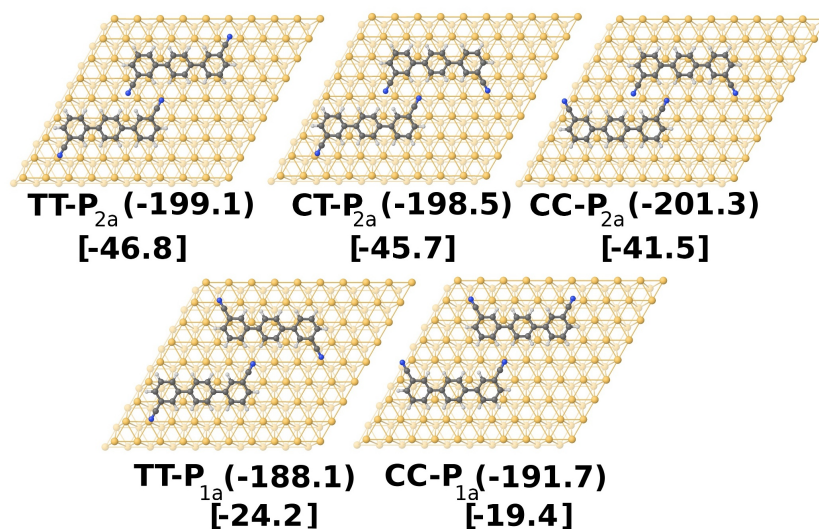


Figure 6 A selection of DFT relaxed dimers on the silver surface together with the corresponding total binding energies per molecule (in round brackets), and H bonding energies (in square brackets), all given in kJ/mol. The legend used to denote the dimers means: the first two characters are composed of either C or T corresponding to the cis or trans conformations of the constituent monomers; the next letter P refers to the parallel form; the index 1 or 2 that follows corresponds to the number of hydrogen bonds in the dimer; finally, a subscript *a* or *b* is used to differentiate between similar structures. More dimers structures are shown in Fig. S6 of the Supplementary Information.

Next we shall consider pTmDC dimers on the silver surface. In total about 25 different dimers, including different orientations of the same dimers, were studied. A number of the most stable dimer structures, fully relaxed with our DFT method, together with their total binding energies per molecule and H bond binding energies (in round and square brackets, respectively) are shown in Fig. 6. The total binding energies of the dimers range from 368.5 to 402.5 kJ/mol and follow the same tendency as in the gas phase⁶ (see also the Supplementary Information).

If we now compare the on-surface dimer total binding energies (around 385 kJ/mol) with binding energies of single monomers (around 192 kJ/mol), and binding energy in the gas phase dimers (around 29 kJ/mol), we see that these are not additive. This is because not all four N atoms of the dimers present NAS-type interactions; for instance, some of the N atoms are located above the Ag hollow sites and hence are less strongly bound to the surface. This is also reflected in the EDD plots (see Fig. S7 in the Supplementary Information).

Looking at the dimer geometries in more detail, we find that the effect of the surface manifests itself in mostly re-orienting the dimers on the surface in such a way as to best stabilize the structure; however, the relative orientation of the molecules in the dimers is very similar to that in the gas phase. We also find that only carbonitrile groups at two ends of dimers remain bent towards the surface (showing NAS interactions similar to what CN-groups in the monomers do), while the CN-groups engaged in the H bonding are practically parallel to the surface, which is likely to be the main cause of the reduction of the binding energies from a mere sum of energies due to different interactions.

To analyze the nature of bonding between the molecules and of the molecules with the surface, we looked at electron density plots (see Fig. S7 in the Supplementary Information). It is seen that docking sites revealing NAS interactions are visible only for some of the N atoms, those which are located above the Ag atoms of the surface. This is consistent with the fact, mentioned above, that the relative interaction of each monomer in the dimers with the surface is somewhat weaker than that for isolated

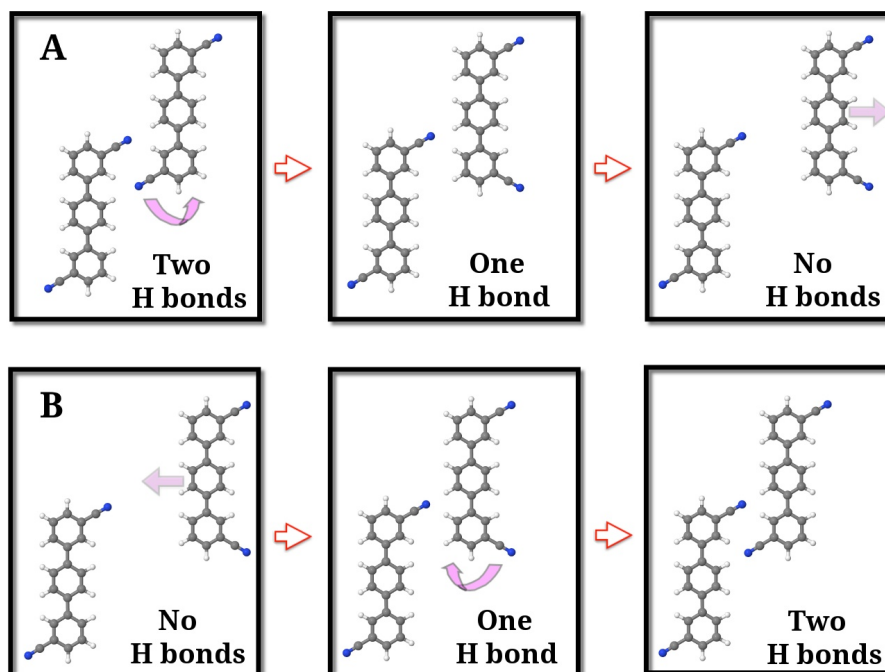


Figure 7 Schematics of the *assisted isomerization* reaction between two molecules on the surface: (A) the right molecule weakens its bonding and detaches from the left molecule increasing the system energy; (B) the right incoming molecule establishes a double H bond with the left molecule reducing the energy of the system.

monomers. Looking at the EDD between two molecules in the dimer, Fig. S7 (B), we find it extremely similar to the one calculated for the same dimer in the gas phase⁶ with the “kebab”-like structure characteristic for the H-bonding between the molecules clearly recognized. Note that the NCI method supports this result as well (Fig. S7, C to F). Detailed analysis confirms that binding between monomers in dimers on the surface can still be characterized in terms of the H-bonding with significant contribution coming from the dispersion interaction (see the Supplementary Information).

As the binding energies of dimers are in the region of 400 kJ/mol, we have not studied their diffusion as a whole, assuming that they are much less mobile than the monomers. However, from the point of view of investigating the growth of the molecular ribbons and linkers observed in,⁵ it is essential to consider possible isomerization of molecules in dimers on the surface. The rationale for this is based on the following observation. Consider a dimer in which two molecules are connected with the double H-bonding, Fig. 7 (A). If one of the benzonitrile groups of a molecule facing the other molecule in a dimer rotates so that the corresponding monomer changes between cis and trans, the interaction between the monomers in the dimer would weaken and either of the molecules may easily diffuse out. Reversely, see Fig. 7 (B), a molecule may come closer to another, establish a single H bond, and then undergo an isomerization reaction which would result in a double H bond between the two, providing the fundamental mechanism for dimer formation on the surface; this dimer may then serve as a nucleus for a further growth. The same type of reaction may also be responsible for the ribbons growth when a monomer comes to an already formed ribbon and then, upon the appropriate isomerization reaction, would attach to it.

For the isomerization reaction between C-T and C-C dimers we have studied both the under-side and upper-side mechanisms (Fig. 8). As expected, this calculation confirms that the upper-side mechanism requires larger energy barriers; hence for the isomerization reaction between T-T and T-C dimers only the under-side mechanism was studied shown in Fig. S8 of the Supplementary Information. In both cases the initial structures correspond to a P_{2a} like structure with the double H bond, while the final structure is the P_{1a} like with only a single bond. The essential result here is that the P_{2a} dimers are by at least 19.3 kJ/mol more favorable than the P_{1a} structures involving either neighboring T or C monomers. Therefore, the energy barrier of 61.7 kJ/mol required to break one H bond in the P_{2a} dimer and turning it into a P_{1a} dimer is by 19.3 kJ/mol larger than the barrier needed for the reverse reaction of turning a P_{1a} dimer into a more stable P_{2a} one. It follows from this consideration, that when two molecules come close to each other to form a favorable arrangement which may facilitate the formation of a proper

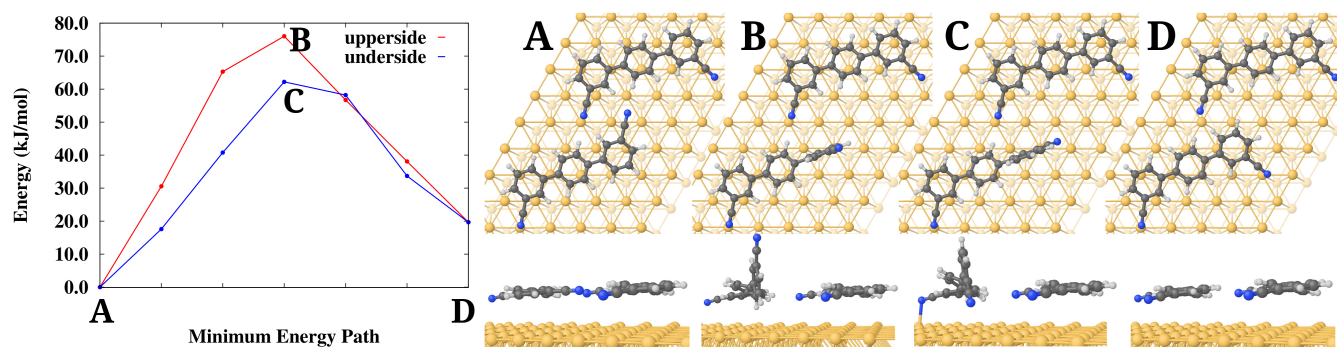


Figure 8 The MEP (the left panel) and the corresponding NEB+DFT relaxed geometries of the initial (A), final (D), and transition states for the upper-side (B) and under-side (C) mechanisms of the cis-assisted isomerization reaction between C-T and C-C dimers.

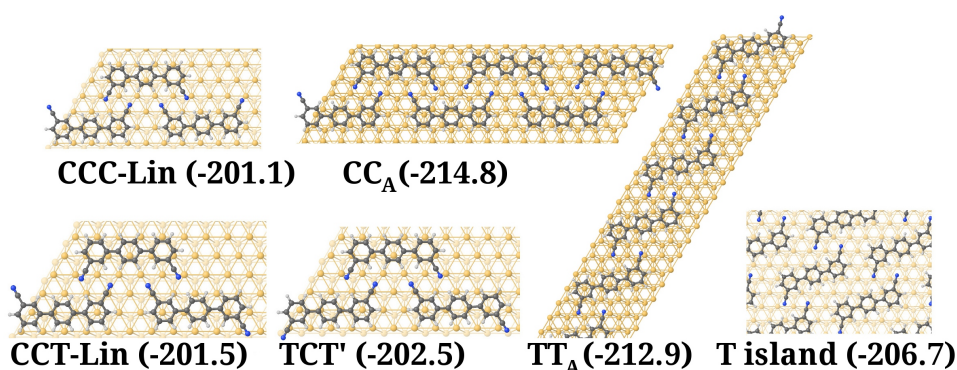


Figure 9 Relaxed geometries and corresponding binding energies (per molecule, in brackets, in kJ/mol) of several linker clusters (CCC-Lin, CCT-Lin and TCT'-Lin), ribbons (CC_A and TT_A) and the T monolayer on the silver surface (top views).

dimer with a double H bond, then the appropriate isomerization reaction would favor such a formation yielding a lower system energy. Hence, if isomerization of monomers, as mentioned above, does not modify significantly the system energy, then the isomerization of molecules arranged next to each others, what we shall call an *assisted isomerization*, will result in a lower free energy of the system.

Linkers and ribbons on the silver surface

Some of the ribbons and linkers considered previously in the gas phase⁶ have also been relaxed on the surface using our DFT method to check their stability.

In the case of periodic ribbons, there is a question of their commensurability with the surface: larger surface cells may need to be taken to accommodate the sufficient number of primitive unit cells of the ribbon structure. In fact, different cells need to be considered to find the structure with the lowest Gibbs free energy. To avoid these rather tedious and expensive computations, we have chosen the smallest cell for the silver surface which accommodates the ribbons at the distances between molecules which are no more than 0.01 Å different from those found in the same ribbons in the gas phase.⁶

The relaxed geometries of two types of ribbons, CC_A and TT_A , consisting of repeated C and T monomers respectively, are shown in Fig. 9 (see also Supplementary Information). The molecules in the ribbons comprise a planar geometry with substantial binding energies (per molecule), also shown in the same Figure. As ribbons have a higher binding energy per molecule than monomers and dimers, it is expected to find molecules aggregated on the surface rather than free molecules or dimers.

We have also considered a number of linker structures composed of 3 molecules which were also placed on the surface and relaxed with DFT. These are shown, together with their binding energies (per molecule) in Fig. 9 (see also Supplementary

Information). All the structures we considered are nearly planar.

The calculations described in this section show that ribbons and linkers are stable on the surface and that their structures are very similar to the ones in the gas phase⁶ confirming that the H-bonding plays the dominant role in the binding mechanism responsible for stability of the molecular aggregates on the silver surface.

Islands on the silver surface

It is known from experiment⁵ that at large coverages the molecules form brickwall type islands. To understand the energetics of the most dense bi-dimensional phase, a 2D monolayer of molecules has also been studied. As in the case of the ribbons, we employed such orientation of the molecules with respect to the surface that allows to have a simultaneous periodicity in both organic and metallic lattices with the smallest unit cell of 4 molecules. The resulting binding energies per molecule are 206.7 kJ/mol for an all trans monolayer and 201.8 kJ/mol for a monolayer formed only by cis molecules. The optimized geometries reveal a nearly planar conformation with a dihedral angle lower than 15° between phenyl rings. The fully relaxed geometry for a T monolayer is shown in Fig. 9. The mean length of the H bond is 2.6 Å and the molecules are at 3.37 Å above the surface. This fact shows that the larger the number of neighbors a molecule has, the higher the molecule is over the surface because the carbonitrile groups tends to participate in the H bonds, although the effect is small.

The T monolayer can be viewed as consisting of TT_A chains placed side-by-side. Since each molecule in the monolayer is double hydrogen bonded to two molecules from the neighboring chains, it would be interesting to investigate whether the molecules remain in their isomerization state at RT or can easily change between T and C states. To this end, we investigated the isomerization reaction for a monomer in the T monolayer and found a barrier of 54.2 kJ/mol for the T→C isomerization via under-side mechanism, and 47.2 kJ/mol for the reverse reaction (Fig. S11 in the Supplementary Information). The relatively low barriers we find for the isomerization reaction in the monolayer imply that islands at RT are composed by a mixture of the three isomers inter-converting continuously one into the other. Actually, in the STM images of the islands⁵ one can see bright bridges between many molecules on both sides of them (see Fig. S12 in the Supplementary Information) implying that indeed these molecules do change their isomerization state frequently on the time scale of the STM scan.

Kinetic Monte Carlo simulations

To model the growth of the assemblies the pTmDC molecules may form on the silver surface, we performed extensive KMC simulations. Because of extremely large number of possible adsorption sites, which would require either introducing a fine grid or performing lattice-free KMC simulations, the problem was considerably simplified to make it tractable. This has been done by introducing two inter-penetrating hexagonal lattices, serving as a grid, and postulating that the molecules may only occupy the sides of the hexagons with their N atoms (or benzonitrile groups) placed on the corresponding vertices of the grid. When a molecule occupies a position on the grid (and there are three independent orientations), it may be in either of the four states, corresponding to two possible orientations of the benzonitrile groups corresponding to C or T isomers, see Fig. 10 (A). Each monomer can interact with its neighbors which may occupy four positions around it as shown in Fig. 10 (B), forming dimers of the kind $XY-P_{na}$, where X and Y can be either C or T and n can be 1 or 2 (see Fig. 6). Note that in real simulations only some of the four neighbors shown in Fig. 10 (B) may be present. For the sake of simplicity, in our KMC simulations we have not taken into account the weaker dimers XY-Tri or $XY-P_{nb}$.

Since we find in our NEB calculations of diffusion of monomers that the main diffusion mechanism is pivoting, the molecules were allowed to move on the grid by using either of their ends as a pivot and rotating with the other end by $\pm 60^\circ$, Fig. 10 (C). Not only the monomers may diffuse on the surfaces on their own, a molecule, if attached to a cluster, may diffuse out (detach from the cluster) to an empty position with the barrier which is calculated as a monomer diffusion barrier plus a sum of the interaction energies of the molecule with all its neighbors. Note that only monomers are allowed to diffuse on the surface, larger clusters (such as dimers, trimers, etc.) cannot move as a whole. By going through the isomerization transition $C \rightleftharpoons T$ the molecules do not change their orientation, but do change their state within the four possibilities shown in Fig. 10 (A). If a molecule is placed next to another, an assisted isomerization is allowed with the corresponding barriers depending on whether initially the molecules are connected by a double or single H bond, see Fig 10 (D and E). Finally, molecules are also allowed to desorb from the surface using their adsorption energy as the energy barrier for this transition. All the moves implemented in our KMC code and the corresponding energy barriers ΔE are schematically shown in Fig.10. Each “move” of the molecule on the grid is associated

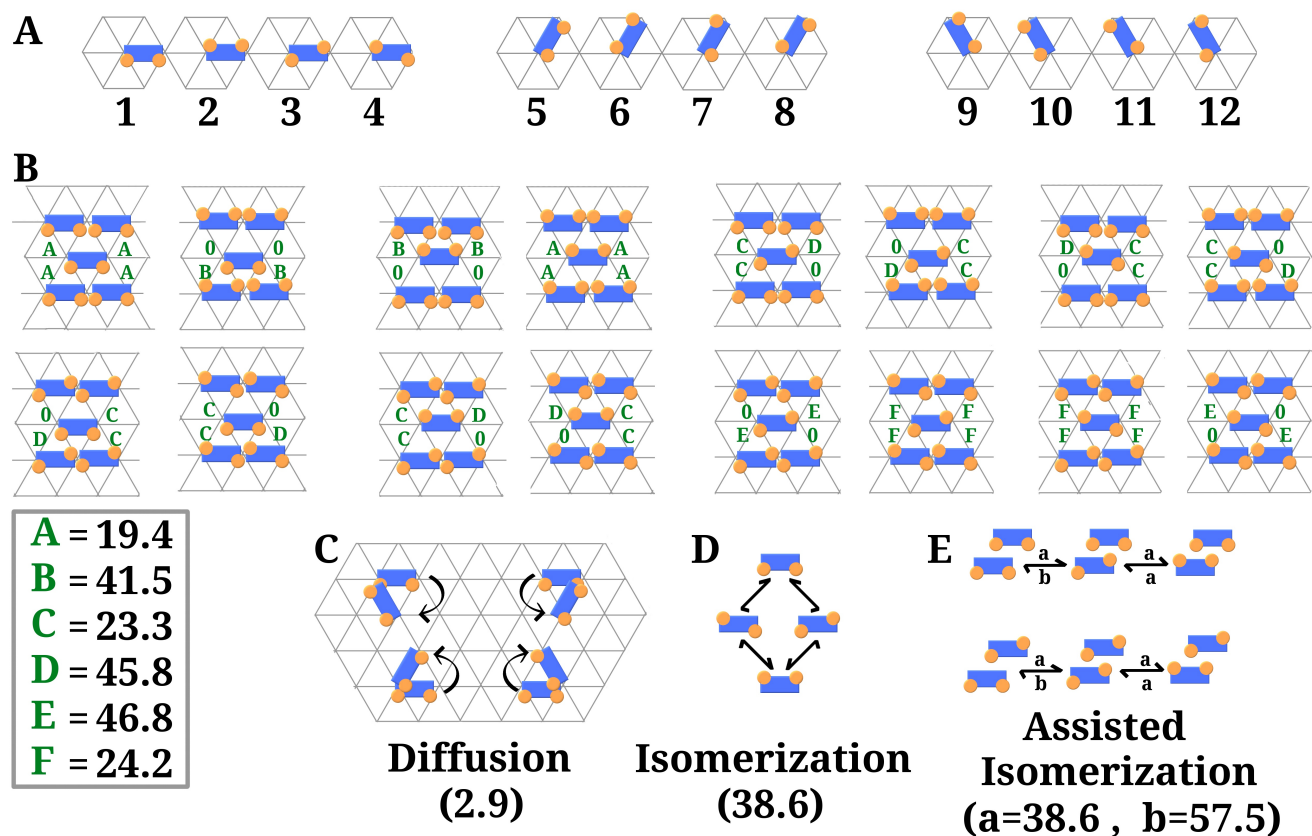


Figure 10 Schematic view of configurations, interactions and moves implemented in the KMC simulation. (A) All 12 possible non-equivalent states of a monomer on the surface. The central point of the hexagon is the net point occupied by the molecule. (B) Various arrangements for a monomer (placed in the center) with its four neighbors (only some may be present in a real simulation). Strength of the pair interactions is indicated with green labels (from A to F), which values were tuned according to our DFT results and are detailed in the light gray box (in kJ/mol). Only shown interactions for monomers 1 to 4. Two more sets of interactions exist by rotating the monomers by 60° (monomers 5 to 8) and 120° (monomers 9 to 12), that yields a total of 192 interactions. (C) The four diffusion mechanisms for a representative monomer. (D) Possible isomerization transformations for an isolated molecule and (E) the assisted isomerization transformations, where the barrier for the reaction “a” is the same as for an isolated monomer and “b” involves the breaking of one H bond. The energy barriers (in brackets) are given in kJ/mol. Blue rectangle represents the aromatic chain of the monomer, orange circles the carbonitrile groups, and the vertices of the hexagonal grid are the Ag atoms of the surface.

with the transition rate $r = \nu e^{-\Delta E/k_B T}$ based on the energy barrier ΔE we have calculated with DFT and the common prefactor $\nu = 10^{13} \text{ s}^{-1}$. Here k_B is the Boltzmann's constant and T the absolute temperature.

In the simulations periodic boundary conditions were implemented with the cell comprising a 85×85 grid. The simulations were run in the following way. To speed up the simulations, either 4 or 5 molecules were initially deposited at random on the grid. These molecules were allowed to perform all possible moves described above. In addition, a deposition of a molecule onto the surface at an arbitrary empty position chosen at random is also allowed with a predefined deposition rate. The deposition is considered as a separate "move" which is attached to the list of all moves. At each KMC step a particular move (diffusion, isomerization, deposition or desorption) is chosen at random using the standard KMC algorithm.^{3,24,25} When a predefined coverage was reached, the deposition was ceased, while all other moves were allowed to continue to be executed until the desired number of KMC steps was reached. Each such simulation was run on average for over 225 million KMC steps using several seed values to accumulate statistics.

Various structures observed in experiment⁵ were frequently seen in our KMC simulations, Fig. 11. Often we observed the molecules starting to condensate in small clusters (or islands), which are surrounded mainly by C monomers pointing its carbonitrile groups towards the interior of the cluster. When one of these molecules at the edges isomerizes to a T or leaves the cluster uncovering a T isomer, a chiral T chain can start growing from the cluster when an equal isomer binds to the first T monomer forming a TT-P_{2a} dimer. Then, in several cases the growth of a chain may be facilitated: (i) similar enantiomers can bind directly to enlarge the chain, (ii) a C monomer can bind to the chain forming a CT-P_{2a} dimer at the end of the chain, and after the isomerization of the free end of the C monomer to yield the T enantiomer, or (iii) a C monomer can form a CT-P_{1a} dimer at the end of the chain followed by the assisted isomerization mechanism yielding the required T enantiomer. Although these chains are relatively stable and can easily be formed, they can be destroyed at room temperature unless are stabilized at both ends by clusters. During the growth of the chains, they can interconnect forming more complex patterns by means of the linkers.

Besides the straight growth, a chain may change its growth direction if a linker is created. This happens if a monomer binds to the chain end formed by a CT-P_{2a} dimer. Then if the new added monomer is: (i) a cis, then a CCT-Lin linker is created, or (ii) if it is a T' (the specular enantiomer of the isomer in the chain), a TCT'-Lin linker happens instead. In the former case a kink is created in the ribbon, which continues growing in the same direction (see Fig. 11 C). In the latter case the direction of growth is changed with molecules tending to aggregate in between both chiral ribbons forming small clusters (see Fig. 11 D). From a kink, a second ribbon adjacent to the main chain can start to grow as is shown in Fig. 11 (F).

As we said above, the borders of islands are mainly formed by C isomers. The growth of these islands is produced in several steps. Firstly, either a new C isomer reaches the borders by diffusion, or a T approaches to the border and then, by means of the assisted isomerization mechanism, becomes a C isomer. It can be stabilized when the monomers in the interior isomerize to create more H bonds with the new added monomer. Those monomers at the edges that are not stabilized by this mechanism are very mobile and can leave the cluster easily. This is in accordance with the experiment, according to which, at submonolayer coverages, supramolecular islands coexist with a disordered fluid phase of highly mobile molecules.⁵

Appearance of long ribbons of molecules after thermal quenching is a characteristic feature in the observed experimental STM images.⁵ We consistently observed formation of such features also in our KMC simulations, Fig. 11. We believe that the growth of long ribbons of trans species happens due to a delicate balance between the strength of the different H bonds and the isomerization barriers. While at room temperature the associated transition rates of breaking any H bond are similar, at lower temperature the rate of breaking a single H bond becomes relatively much larger than the rate for breaking a double H bond. Furthermore, isomerization of monomers involving the breaking of an H bond at the edges of the islands are much more difficult to occur than at the free end of the monomers at the ends of chains. This makes it more difficult to trap new monomers, by the mechanisms explained above, at the edges of the islands than at the ends of chains, favoring the growth of the chiral ribbons with a T isomer proportion increasing.

Other features observed experimentally⁵ such as linkers, kinks, clusters and islands were also consistently observed in our KMC simulations, Fig. 11. We have also observed formation of islands when performing simulations at higher coverages (see details in the Supplementary Information).

It was claimed in⁵ that the number of T isomers on the surface greatly surpassed that of the C isomers. We did not find this in our simulations: at room temperature all our simulations yield a slightly bigger proportion of C isomers with a mean value of 55.4%, while the L-trans and D-trans isomers were found at 22.5% and 22.1%, respectively. At lower temperatures (assuming the same deposition rate), the proportion of C isomers decreased to 42.7%, whereas T isomers were found in increasing numbers (around 29.2% for L-trans and 28.7% for the D-trans). This final result suggests that a separate detailed investigation would be of utility to explore if supramolecular arrangements of pTmDC on silver (111) surface with different C-T composition can be

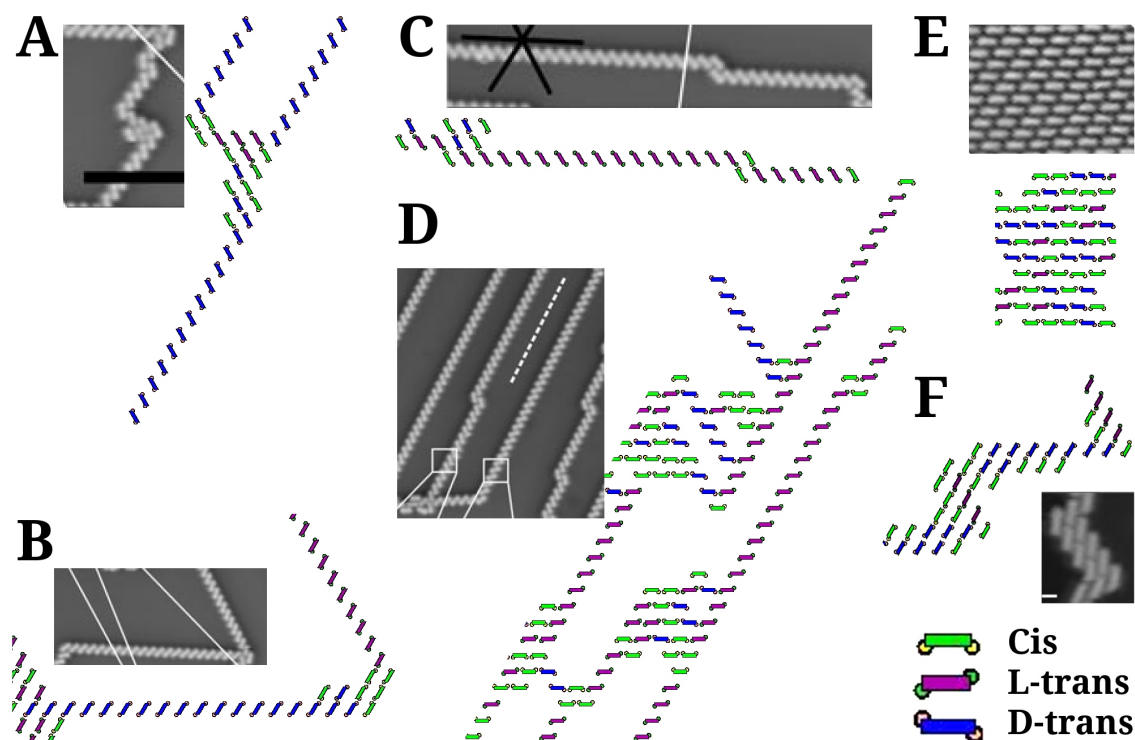


Figure 11 Sections of the 85x85 KMC simulation cell corresponding to a 20% coverage and a 10^{-7} ps $^{-1}$ deposition rate are compared with experimental STM images (adapted with permission from Ref. 5). The experimental STM high-resolution image used for A, B, C, D and F was taken at 8 K on Ag(111) with a coverage of 0.1 ML, and STM image in E was taken at room temperature. A, B and C STM images have been horizontally mirrored to facilitate the comparison with the structures found in the simulations. (A) A long chiral chain formed by D-trans, with some molecules aggregated around a kink. It is also seen that a CCC-Lin linker binds a long L-trans with a short D-trans chain. (B) Two long chains of the two different isomers bound by a double CCC-Lin linker. (C) A long chiral chain formed by L-trans with a TCC-Lin linker in the middle forming a kink. (D) Long parallel chains with all kinds of linkers; note that it is seen in the example provided that clusters may condense between chains in our KMC simulations. (E) A small piece of an island formed by a mixture of both C and T isomers. (F) Side-by-side chains growing from linkers. Green rectangles represent cis, blue D-trans, and magenta L-trans isomers. The snapshots A, B and C correspond to the step 198000000 of simulation number 01 that was run at 200 K, snapshots D and E were taken from the step 755000000 of the simulation number 02 run at 175 K, and F was taken from the step 760000000 of the simulation 03 run at 300 K. The movies of these KMC simulations are given in the Supplementary Information.

found as the temperature is gradually decreased.

Conclusions

In this paper we considered the kinetics of growth at small and intermediate coverages of assemblies of pTmDC molecules on the Ag(111) surface. We have used a toolkit of methods, from DFT modeling of adsorption geometries and NEB calculations of diffusion and isomerization energy barriers and mechanisms, to KMC modeling of the actual growth of assemblies. It was found that the dispersion interaction is the main contributor that binds the molecular assemblies to the surface with particularly favored adsorption sites through NAS interactions in which N atoms are placed above surface Ag atoms. This naturally leads to a slightly corrugated surface landscape for the molecules. Also, the preferred sites are those where phenyl rings avoid Ag atoms underneath. The molecule can be viewed as standing on two legs. The fact that the dispersion contribution dominates molecule-surface interactions leads to the molecules being quite mobile on the surface at RT and diffuse exploiting the pivoting mechanism when one “leg” serves as a pivot while another moves to the new available site. We also investigated possibilities of interconversion of C and T isomers into each other on the surface. We find that monomers may easily undergo transformations

into each other following the under-side mechanism which ensures the lowest energy barrier; moreover, the transformation occurs with equal rates implying equal amounts of both C and T monomers on the surface.

However, as molecules come closer to each other, they bind via a hydrogen bonding interaction forming dimers, chains, clusters and linkers. These structures were found to be almost identical to those found in our previous gas phase DFT calculations.⁶ We find that H bonds are up to 1.5 times stronger on the surface than in the gas phase and this proves the dominant role the H bonding plays in binding the molecules together in the observed assemblies.⁵ At the same time, we find that the growth is greatly facilitated by the assisted isomerization mechanism. Of course, lowering of the system free energy due to formation of H bonds between molecules is the main driving force behind the assembly formation. However, the assisted isomerization mechanism is the key mechanism of growth of linkers, islands and long ribbons. This is because it leads to maximizing the number of double H bonds between molecules. Hence, this specific mechanism is capable of explaining the structures observed in the experiment.⁵

In our KMC simulations, we find that during the growth process chiral ribbons are created and destroyed at room temperature and can interconnect between themselves, creating more complex patterns by means of the linkers, where small clusters start to condensate. At the ends of the ribbons is a monomer with a free end that can isomerize easily facilitating further growth. At submonolayer coverages supramolecular islands coexist with a disordered fluid phase of highly mobile monomers as was also observed in the experiment.⁵

Importantly, no evidence was found in our theoretical investigation on the alleged chiral selectivity related to abundance of the T isomers upon the assembly as was suggested in,⁵ the claim which was made entirely on analyzing the STM images. Instead, we find that both isomers are present almost in equal amounts. Moreover, islands are suggested to be not static: they are in a dynamic equilibrium whereby the three isomers (C and both T isomers) interconvert one into the other continuously at RT. However, the edges of islands are formed mainly by cis isomers.

Our study shows the importance of theoretical modeling in making conclusions concerning observed assemblies and the mechanisms responsible for their growth. We hope that this investigation sheds light on the mechanism of self-assembly of pTmDC molecules on the Ag(111) surface, demonstrating clearly, on the one hand, the role of their interaction with the surface which provides their high mobility via the pivoting mechanism, and, on the other, establishes the relevance of the assisted isomerization reaction which are the key for understanding the observed supramolecular assemblies. This detailed atomistic self-assembly mechanism may be behind the growth of many other hydrogen bonding structures of chiral molecules.

Acknowledgment

D.A.-P. and J.M.R. acknowledge support by the Spanish MINECO and the ERDF of the European Union (project no. CTQ2012-38599-C02). We belong to the MALTA Team (CSD2007-0045 project, MEC Consolider Ingenio 2010 program). D.A.-P. thanks the now extinct Spanish MICINN for an FPI grant. Via our membership of the UK's HPC Materials Chemistry Consortium, which is funded by EPSRC (EP/F067496), this work made use of the facilities of HECToR, the UK's national high-performance computing service, which is funded by the Office of Science and Technology through EPSRC's High End Computing Programme. MALTA computational facilities are also acknowledged.

References

- [1] J. V. Barth, G. Costantini and K. Kern, *Nature*, 2005, **437**, 671–679.
- [2] A. Bandyopadhyay, R. Pati, S. Sahu, F. Peper and D. Fujita, *Nat. Phys.*, 2010, **6**, 369–375.
- [3] M. Mura, F. Silly, V. Burlakov, M. R. Castell, G. A. D. Briggs and L. N. Kantorovich, *Phys. Rev. Lett.*, 2012, **108**, 176103.
- [4] S. M. Barlow and R. Raval, *Surf. Sci. Rep.*, 2003, **50**, 201–341.
- [5] M. Marschall, J. Reichert, K. Seufert, W. Auwärter, F. Klappenberger, A. Weber-Bargioni, S. Klyatskaya, G. Zoppellaro, A. Nefedov, T. Strunskus, C. Wöll, M. Ruben and J. V. Barth, *ChemPhysChem*, 2010, **11**, 1446–1451.
- [6] D. Abbasi-Pérez, J. M. Recio and L. Kantorovich, *J. Phys. Chem. C*, 2014, **118**, 10358–10365.

- [7] H. Jónsson, G. Mills and K. W. Jacobsen, in *Classical and Quantum Dynamics in Condensed Phase Simulations*, ed. B. J. Berne, G. Ciccotti and D. F. Coker, World Scientific, 1998, ch. Nudged Elastic Band Method for Finding Minimum Energy Paths of Transitions.
- [8] G. Mills, H. Jónsson and G. K. Schenter, *Surf. Sci.*, 1995, **324**, 305–337.
- [9] J. VandeVondele, M. Krack, F. Mohamed, M. Parrinello, T. Chassaing and J. Hutter, *Comput. Phys. Commun.*, 2005, **167**, 103 – 128.
- [10] G. Lippert, H. Jurg and M. Parrinello, *Mol. Phys.*, 1997, **92**, 477–488.
- [11] S. Goedecker, M. Teter and J. Hutter, *Phys. Rev. B*, 1996, **54**, 1703–1710.
- [12] J. P. Perdew, K. Burke and M. Ernzerhof, *Phys. Rev. Lett.*, 1996, **77**, 3865–3868.
- [13] S. Grimme, J. Antony, S. Ehrlich and H. Krieg, *J. Chem. Phys.*, 2010, **132**, 154104.
- [14] J. VandeVondele and J. Hutter, *J. Chem. Phys.*, 2007, **127**, 114105.
- [15] S. Boys and F. Bernardi, *Mol. Phys.*, 1970, **19**, 553.
- [16] G. Henkelman and H. Jónsson, *J. Chem. Phys.*, 2000, **113**, 9978–9985.
- [17] G. Henkelman, B. P. Uberuaga and H. Jónsson, *J. Chem. Phys.*, 2000, **113**, 9901–9904.
- [18] R. Otero, M. Schock, L. M. Molina, E. Legsgaard, I. Stensgaard, B. Hammer and F. Besenbacher, *Angew. Chem. Int. Ed.*, 2005, **44**, 2270.
- [19] R. E. A. Kelly and L. Kantorovich, *J. Mater. Chem.*, 2006, **16**, 1894–1905.
- [20] M. Mura, A. Gulans, T. Thonhauser and L. Kantorovich, *Phys. Chem. Chem. Phys.*, 2010, **12**, 4759–4767.
- [21] E. R. Johnson, S. Keinan, P. Mori-Sánchez, J. Contreras-García, A. J. Cohen and W. Yang, *J. Am. Chem. Soc.*, 2010, **132**, 6498–6506.
- [22] J. Contreras-García, W. Yang and E. R. Johnson, *J. Phys. Chem. A*, 2011, **115**, 12983–12990.
- [23] J. Contreras-García, M. Calatayud, J.-P. Piquemal and J. Recio, *Comput. Theor. Chem.*, 2012, **998**, 193 – 201.
- [24] A. F. Voter, in *Radiation effects in solids*, ed. K. E. Sickafus, E. A. Kotomin and B. P. Uberuaga, Springer, NATO Publishing Unit, Dordrecht, The Netherlands, 2005.
- [25] K. Reuter, C. Stampfl and M. Scheffler, in *Ab initio Atomistic Thermodynamic and Stastical Mechanics of Surface Properties and Functions*, ed. S. Yip, Springer, 2005, vol. Part A, p. 149.